DMD Fast Forward. Published on November 19, 2019 as DOI: 10.1124/dmd.119.088898
This article has not been copyedited and formatted. The final version may differ from this version.

1. Title Page

Mechanistic Modeling of the Hepatic Disposition of Estradiol-17β-Glucuronide in Sandwich-Cultured Human Hepatocytes

Katsuaki Ito *, Noora Sjöstedt * and Kim L.R. Brouwer

Division of Pharmacotherapy and Experimental Therapeutics, UNC Eshelman School of Pharmacy, University of North Carolina at Chapel Hill, Chapel Hill, NC (K.I., N.S., K.L.R.B.); DMPK Research Department, Teijin Pharma Limited, Hino, Tokyo, Japan (K.I.)

*Authors contributed equally to the manuscript

2. Running Title Page

a) Running Title (56 out of 60 characters including spaces): $E_2$17G disposition in sandwich-cultured human hepatocytes

b) Corresponding author: Kim L.R. Brouwer, UNC Eshelman School of Pharmacy, University of North Carolina at Chapel Hill, CB #7569, Chapel Hill, NC 27599-7569. Phone: (919) 962-7030. Fax: (919) 962-0644. E-mail address: kbrouwer@unc.edu.

c) Number of text pages: 33

Number of tables: 2

Number of figures: 5

Number of references: 47

Number of words in the Abstract: 249 out of 250

Number of words in the Introduction: 676 out of 750

Number of words in the Discussion: 1467 out of 1500

d) Abbreviations: BEI, biliary excretion index; $CL_{int,bile}$, intrinsic biliary excretion clearance; $CL_{int,BL}$, intrinsic basolateral efflux clearance; CL_{uptake}, uptake clearance; $E_2$17G, estradiol-17β-glucuronide; HBSS, Hanks' balanced salt solution; ICP, intrahepatic cholestasis of pregnancy; K_{flux}, rate constant for flux from bile into the medium; MRP, multidrug resistance-associated protein; OATP, organic anion transporting polypeptide; SCHH, sandwich-cultured human hepatocytes; TCA, taurocholate

Section: Metabolism, Transport, and Pharmacogenomics

3. Abstract

Estradiol-17β-glucuronide ($E_2$17G) is an estrogen metabolite that has cholestatic properties. In humans, circulating $E_2$17G is transported into hepatocytes by organic anion transporting polypeptides (OATPs) and is excreted into bile by multidrug-resistance associated protein 2 (MRP2). $E_2$17G is also a substrate of the basolateral efflux transporters MRP3 and MRP4, which translocate $E_2$17G from hepatocytes to blood. However, the contribution of basolateral efflux to hepatocyte disposition of $E_2$17G has not been evaluated previously. To address this question, $E_2$17G disposition was studied in sandwich-cultured human hepatocytes and mechanistic modeling was applied to calculate clearance values (mean ± SD) for uptake, intrinsic biliary excretion ($CL_{int,bile}$) and intrinsic basolateral efflux ($CL_{int,BL}$). The biliary excretion index (BEI) of $E_2$17G was 45 ± 6%. The $CL_{int,BL}$ of $E_2$17G (0.18 ± 0.03 ml/min/g liver) was 1.6-fold higher than $CL_{int,bile}$ (0.11 ± 0.06 ml/min/g liver). Simulations were performed to study the effects of increased $CL_{int,BL}$ and a concomitant decrease in $CL_{int,bile}$ on hepatic $E_2$17G exposure. Results demonstrated that increased $CL_{int,BL}$ can effectively reduce hepatocellular and biliary exposure to this potent cholestatic agent. Simulations also revealed that basolateral efflux can compensate for impaired biliary excretion, and vice versa, to avoid accumulation of $E_2$17G in hepatocytes. However, when both clearance processes are impaired by 90%, hepatocyte $E_2$17G exposure increases up to 10-fold. These data highlight the contribution of basolateral efflux transport, in addition to MRP2-mediated biliary excretion, to $E_2$17G disposition in human hepatocytes. This elimination route could be important, especially in cases where basolateral efflux is induced, such as cholestasis.

4. Significance Statement (max 80 words)

The disposition of the cholestatic estrogen metabolite estradiol-17β-glucuronide ($E_2$17G) was characterized in sandwich-cultured human hepatocytes. The basolateral efflux clearance was estimated to be 1.6-fold higher than the biliary excretion clearance, emphasizing the contribution of basolateral elimination in addition to biliary excretion. Simulations highlight how hepatocytes can effectively cope with increased $E_2$17G through the regulation of both basolateral and biliary transporters.

5. Visual Abstract (please see supplemental file)

DMD Fast Forward. Published on November 19, 2019 as DOI: 10.1124/dmd.119.088898
This article has not been copyedited and formatted. The final version may differ from this version.

6. Introduction

Estradiol-17β-glucuronide ($E_2$17G) is a metabolite of estradiol, an estrogen steroid hormone. $E_2$17G is formed by uridine 5'-diphospho-glucuronosyltransferase (UGT) 2B7-mediated glucuronidation of estradiol, primarily in the liver (Musey et al., 1997). Hepatic concentrations of $E_2$17G are regulated by multiple transport proteins expressed in the liver. $E_2$17G is a well-known substrate of multidrug-resistance associated protein 2 (MRP2, ABCC2), which mediates $E_2$17G excretion into bile (Morikawa et al., 2000). On the basolateral (sinusoidal) membrane, organic anion transporting polypeptides 1B1 and 1B3 (OATP1B1, SLCO1B1 and OATP1B3, SLCO1B1) mediate the uptake of $E_2$17G into hepatocytes from the blood (Karlgren et al., 2012). In fact, $E_2$17G is commonly used as a probe substrate in OATP1B1/1B3 and MRP2 inhibition studies *in vitro* (Pedersen et al., 2008; Karlgren et al., 2012; Brouwer et al., 2013; Morgan et al., 2013). In addition, $E_2$17G is transported by MRP3 (ABCC3) and MRP4 (ABCC4), which pump substrates from hepatocytes into sinusoidal blood on the basolateral membrane (Zeng et al., 2000; Chen et al., 2001). However, the contribution of basolateral efflux to the hepatic disposition of $E_2$17G has not been elucidated.

$E_2$17G transport is of interest because it is a potent cholestatic agent and it is postulated to be involved in the pathogenesis of intrahepatic cholestasis of pregnancy (ICP). ICP is a condition that is characterized by fairly harmless pruritus and elevated serum bile acid concentrations in the mother, but can increase the risk for preterm labor or even intrauterine death (Geenes and Williamson, 2009). Maternal symptoms typically present in the third trimester of pregnancy, coinciding with the highest estrogen levels during pregnancy. Therefore, it is thought that elevated hepatic $E_2$17G concentrations may play a role in triggering ICP. Understanding the mechanisms underlying the hepatic disposition of $E_2$17G is important from the viewpoint of preventing and managing ICP.

DMD Fast Forward. Published on November 19, 2019 as DOI: 10.1124/dmd.119.088898
This article has not been copyedited and formatted. The final version may differ from this version.

Most of the studies regarding the cholestatic effects of $E_2$17G have been performed in rats. $E_2$17G administration (2 µmol infused over 18 min) decreased bile flow by 51% in perfused rat livers (Huang et al., 2000). Additionally, $E_2$17G decreased the elimination of the hepatobiliary imaging agent indocyanine green in female rhesus monkeys (Slikker et al., 1983). MRP2 seems to play a key role in $E_2$17G-induced cholestasis, because even doses 12-fold higher than the dose required for cholestatic effects in wild-type rats did not decrease bile flow in Mrp2-deficient TR^- rats (Huang et al., 2000). Studies in Mrp2-deficient rats have shown that Mrp2 mediates the secretion of glutathione into bile and that this is important for bile acid-independent bile flow (Takikawa et al., 1991; Elferink and Groen, 2002). Overall, $E_2$17G appears to exert its cholestatic effects through several mechanisms. Administration of $E_2$17G to rats increased the internalization of Mrp2 and the bile salt export pump (Bsep) from the cell membrane by clathrin-mediated endocytosis (Mottino et al., 2002; Miszczuk et al., 2018). In addition, $E_2$17G increased the accumulation of bile acids in hepatocytes through trans-inhibition of BSEP (Stieger et al., 2000; Vallejo et al., 2006). This increase in intrahepatic bile acid concentrations could induce organic solute transporter α/β (OSTα/β) expression (Boyer et al., 2006) and enhance bile acid efflux into the blood, which might explain the observed increase in serum bile acids in ICP (Walker et al., 2002).

Although the current literature suggests a possible role for MRP2 in $E_2$17G-induced ICP, as discussed above, several mechanisms appear to be involved in the development of ICP, and MRP2 is not the only process regulating hepatic $E_2$17G exposure. The exposure also is affected by hepatic basolateral uptake and efflux transporters. Therefore, in this study, the contribution of basolateral efflux in the hepatic disposition of $E_2$17G was quantitatively evaluated by uptake and efflux studies using sandwich-cultured human hepatocytes (SCHH) and mechanistic modeling. The clearance estimates derived from the model were used to simulate conditions resulting in inhibition or induction of the different pathways affected by cholestasis or drug-drug interactions based on previously published literature. The results of this study reinforce the notion that

DMD Fast Forward. Published on November 19, 2019 as DOI: 10.1124/dmd.119.088898
This article has not been copyedited and formatted. The final version may differ from this version.

basolateral efflux can act as an important excretion route for $E_2$17G, especially in cholestatic conditions where basolateral transporters (e.g., MRP3, MRP4) are up-regulated.

7. Materials and Methods

Materials

Transporter Certified™ cryopreserved human hepatocytes (3 female donors, Table 1) were obtained from ThermoFisher Scientific (Waltham, MA) and In Vitro ADMET Laboratories (Columbia, MD). QualGro™ Seeding medium and QualGro™ Hepatocyte Culture medium were obtained from BioIVT (Durham, NC). Tritium-labeled estradiol-17β-glucuronide ([^{3}H]-$E_2$17G) (52.9 Ci/mmol, radiochemical purity >97%) and taurocholate ([^{3}H]-TCA) (9.7 Ci/mmol, radiochemical purity > 97%) were purchased from PerkinElmer (Boston, MA). Non-labeled $E_2$17G and TCA were purchased from Sigma-Aldrich (St. Louis, MO). Standard Hank's Balanced Salt Solution (HBSS) and HBSS without calcium and magnesium were purchased from ThermoFisher Scientific (Waltham, MA). Collagen (type I) coated BioCoat 24-well cell culture plates and Matrigel® were obtained from BD Biosciences (San Jose, CA).

Sandwich-cultured human hepatocytes

On day 0, human hepatocytes from the three donors were seeded on BioCoat 24-well plates at a density of 0.45 x 10^6 hepatocytes per well using QualGro™ Seeding Medium, and overlaid with Matrigel® diluted in QualGro™ Hepatocyte Culture Medium (0.25 mg/ml) on day 1. SCHH were maintained in QualGro™ Hepatocyte Culture Medium, which was changed daily until experiments were performed on day 5.

Disposition of $E_2$17G in SCHH

The uptake and efflux studies were conducted by applying B-CLEAR® technology (BioIVT, Durham, NC) according to the schemes shown in Figure 1 (Liu et al., 1999). Briefly, SCHH were washed twice and pre-incubated for 10 min at 37°C with either standard HBSS (containing calcium and magnesium) or Ca^{2+}-free HBSS (HBSS without calcium and magnesium, supplemented with 1 mM EGTA). After pre-incubation, the uptake phase was initiated by

DMD Fast Forward. Published on November 19, 2019 as DOI: 10.1124/dmd.119.088898
This article has not been copyedited and formatted. The final version may differ from this version.

incubating SCHH with 0.3 μM [^{3}H]-$E_2$17G (2 μCi/ml) in standard HBSS at 37°C. $E_2$17G accumulation in cells and biliary networks (cells+bile; measured in SCHH pre-incubated with standard HBSS) and $E_2$17G accumulation in cells (measured in SCHH pre-incubated with Ca^{2+}-free HBSS) was determined during the uptake phase by terminal sampling at designated time points. After the 10-min uptake phase, buffers containing $E_2$17G were removed from the wells, and cells were washed three times with 37°C standard or Ca^{2+}-free HBSS buffer followed by initiation of the efflux phase. During the efflux phase, $E_2$17G efflux into the buffer and the amount remaining in cells and biliary networks (standard HBSS pre-incubation) and cells (Ca^{2+}-free HBSS pre-incubation) were determined by terminal sampling at designated time points. In addition, B-CLEAR® studies were performed as above with taurocholate (TCA) for comparison with the $E_2$17G results. In these studies, SCHH were incubated with 1 μM TCA (0.8 μCi/ml) for 10 min in standard HBSS after a 10-min pre-incubation in standard HBSS or Ca^{2+}-free HBSS. Accumulation of TCA in the cells and cells+bile was determined by terminal sampling.

The radioactivity in samples from cells, cells+bile, and buffer was quantified by liquid scintillation counting using a Tri-Carb 3100TR counter (Perkin Elmer). Prior to analysis, cells were lysed with lysis solution containing 1 X phosphate buffered saline with 0.5% Triton X-100. Total protein concentration of the cell lysates was determined using the Pierce™ BCA Protein Assay Kit (ThermoFisher Scientific). The amount of $E_2$17G and TCA measured in the cell and the buffer samples was normalized to the protein amount in the wells. The biliary excretion index (BEI) was calculated from data at the end of the 10-min uptake phase using equation 1:

$$BEI\ (\%) = \frac{X_{cells+bile} - X_{cells}}{X_{cells+bile}} \times 100 \qquad (1)$$

where $X_{cells+bile}$ is the amount of test compound ($E_2$17G or TCA) accumulated in the cells and bile networks in standard HBSS, and X_{cells} is the amount of test compound accumulated in the cells that were preincubated in Ca^{2+}-free HBSS.

DMD Fast Forward. Published on November 19, 2019 as DOI: 10.1124/dmd.119.088898
This article has not been copyedited and formatted. The final version may differ from this version.

Mechanistic modeling of $E_2$17G in SCHH

Mechanistic modeling was applied to the uptake and efflux data using Phoenix WinNonlin, v7.0 (Certara USA, Princeton, NJ) using a previously reported approach (Pfeifer et al., 2013). Briefly, the mechanistic model depicted in Figure 1 was fit simultaneously to the $E_2$17G uptake and efflux in standard and Ca^{2+}-free HBSS vs. time data. The basolateral uptake clearance (CL_{uptake}), intrinsic basolateral efflux clearance ($CL_{int,BL}$), intrinsic biliary excretion clearance ($CL_{int,bile}$) and the first-order rate constant for flux from the bile network into the buffer (K_{flux}) were determined. Assuming non-saturable clearances for all the pathways, the model equations are as follows:

Mass of $E_2$17G in standard HBSS (X^+_{buffer}):

$$\frac{dX^+_{buffer}}{dt} = C^+_{cells} \times CL_{int,BL} + X_{bile} \times K_{flux} - C^+_{buffer} \times CL_{uptake} - X^+_{buffer} \times K_{wash} \quad (2)$$

Mass of $E_2$17G in Ca^{2+}-free HBSS (X^-_{buffer}):

$$\frac{dX^-_{buffer}}{dt} = C^-_{cells} \times CL_{int,BL} - C^-_{buffer} \times CL_{uptake} - X^-_{buffer} \times K_{wash} + C^-_{cells} \times CL_{int,bile} \quad (3)$$

Mass of $E_2$17G in cells (X_{cells}):

$$\frac{dX_{cells}}{dt} = C_{buffer} \times CL_{uptake} - C_{cells} \times (CL_{int,BL} + CL_{int,bile}) \quad (4)$$

Mass of $E_2$17G in bile (X_{bile}):

$$\frac{dX_{bile}}{dt} = C_{cells} \times CL_{int,bile} - X_{bile} \times K_{flux} \quad (5)$$

Mass of $E_2$17G in cells + bile ($X_{cells+bile}$):

$$\frac{dX_{cells+bile}}{dt} = \frac{X_{bile}}{dt} + \frac{X_{cells}}{dt} \quad (6)$$

DMD Fast Forward. Published on November 19, 2019 as DOI: 10.1124/dmd.119.088898
This article has not been copyedited and formatted. The final version may differ from this version.

The first-order rate constant K_{wash} was fixed at 10^4 min^{-1} between 10 and 11 min in the simulations. This parameter was included to remove all $E_2$17G from the buffer and mimic the wash step between the uptake and efflux phases (Pfeifer et al., 2013; Yang et al., 2015). The initial mass of $E_2$17G in both buffers was set equal to the dose, and the initial mass in the other compartments was set equal to zero. The *in vitro* observations used for data fitting were $E_2$17G $X_{cells+bile}$ and X^+_{buffer} in standard HBSS, and X_{cells} and X^-_{buffer} in Ca^{2+}-free conditions. An additive error model was used for the mass of $E_2$17G in standard HBSS and in cells incubated in Ca^{2+}-free buffer, and a Poisson error model (a power model with a coefficient of 0.5) was used for the other observations. The initial estimate for CL_{uptake} was calculated using the first three time points in the uptake phase as $(dX_{cells+bile}/dt)/C_{buffer}$. The total efflux clearance ($CL_{int,BL}$ + $CL_{int,bile}$) was estimated from efflux phase data under Ca^{2+}-free conditions, where ($CL_{int,bile}$ + $CL_{int,BL}$) = $X^-_{Buffer,21min}$/area under the curve $(AUC)_{cells,11–21min}$. Initial estimates were derived by dividing $CL_{int,bile}$ + $CL_{int,BL}$ by 2. The ordinary differential equations (ODEs) were solved using the matrix exponent ODE solver in Phoenix WinNonlin. The goodness of fit was evaluated based on visual observation of predicted and observed $E_2$17G mass and the CV% of the derived parameters. The model derived clearance values were scaled to the liver and expressed as ml/min/g liver, assuming a protein content of 90 mg protein/g liver (Sohlenius-Sternbeck, 2006). The fraction excreted by the two elimination pathways (fe_{bile} and $fe_{efflux,BL}$) were calculated as the ratio of the specific clearance pathway divided by the sum of both clearance values (Zamek-Gliszczynski et al., 2009).

Effect of transporter induction and inhibition

The effect of transporter induction on $E_2$17G disposition was evaluated by simulating disposition in SCHH using the average clearance estimates derived from the mechanistic modeling. Simulations were performed using Stella version 9 (Isee Systems Inc, Lebanon, NH, USA) and equations 2 - 6. $CL_{int,bile}$ was decreased and $CL_{int,BL}$ was increased by 2- and 4-fold in the simulations. These values were chosen to represent plausible changes in protein levels based on

DMD Fast Forward. Published on November 19, 2019 as DOI: 10.1124/dmd.119.088898
This article has not been copyedited and formatted. The final version may differ from this version.

available literature (Thakkar et al., 2017). The BEI was calculated for each of the simulations using equation 1 and simulated $E_2$17G amounts after 10-min uptake. Simulations (up to 60 min) were performed to evaluate the changes in $E_2$17G in the cells and bile compartments at steady-state due to transporter induction. In addition, the effect of inhibition of $CL_{int,bile}$ and/or $CL_{int,BL}$ on $E_2$17G accumulation at steady-state was calculated using equation 7 and varying the clearance values:

$$K_p = \frac{CL_{uptake}}{CL_{int,BL}+CL_{int,bile}} \quad (7)$$

where K_p is the hepatocyte to buffer concentration ratio. All data from the simulations and K_p calculations were normalized to control values (no inhibition or induction) and presented as fold-change.

8. Results

All three hepatocyte lots showed time-dependent accumulation of $E_2$17G into cells during the uptake phase and excretion into the buffer during the efflux phase (Figure 2). The biliary excretion index (BEI) of $E_2$17G after 10-min uptake was 40 – 52% in the three lots (Figure 3). The functionality of the hepatocyte lots was verified with TCA; the BEI of TCA in the same hepatocyte lots was 41 – 62%. All of the observed time course data for $E_2$17G uptake and efflux were described adequately by the model and the CVs of the derived parameters were ≤ 68%. The largest variability in parameter estimates between lots was seen for $CL_{int,bile}$ (55% CV between lots). The average value of $CL_{int,BL}$ (0.18 ± 0.03 ml/min/g liver) was 1.6-fold higher than $CL_{int,bile}$ (0.11 ± 0.06 ml/min/g liver)(Table 2). The average fraction of $E_2$17G excreted via basolateral efflux ($fe_{efflux,BL}$) was 61%, and 39% was excreted via biliary excretion (fe_{bile}).

Sensitivity analysis revealed that hepatic $E_2$17G exposure is sensitive to $CL_{int,BL}$; a 64% decrease in hepatic $E_2$17G exposure was observed when basolateral efflux was increased by 4-fold (Fig. 4A). A decrease in $CL_{int,bile}$ caused an increase in hepatic $E_2$17G exposure, especially when $CL_{int,BL}$ was unchanged. However, when $CL_{int,BL}$ was simultaneously increased 4-fold, even a 4-fold reduction in $CL_{int,bile}$ had minimal effects on $E_2$17G in hepatocytes. $E_2$17G in bile was decreased to a similar extent by a 2-fold increase in $CL_{int,BL}$ and a 2-fold decrease in $CL_{int,\ bile}$ (Fig. 4B). The same was true for a 4-fold increase in $CL_{int,BL}$ and a 4-fold decrease in $CL_{int,\ bile}$ (Fig. 4B).

The maximal simulated decrease in biliary $E_2$17G was 90%, which was achieved with a 4-fold increase in $CL_{int,BL}$ and a 4-fold decrease in $CL_{int,bile}$. The BEI was only marginally affected by changes in $CL_{int,BL}$; the BEI of $E_2$17G was decreased by more than 30% when $CL_{int,bile}$ was reduced 2-fold and more than 60% when $CL_{int,bile}$ was reduced 4-fold (Fig 4C).

The results of simulations to evaluate the impact of inhibition of biliary excretion and/or basolateral efflux of $E_2$17G on hepatic exposure are plotted in Fig. 5. As shown, only modest changes (under

DMD Fast Forward. Published on November 19, 2019 as DOI: 10.1124/dmd.119.088898
This article has not been copyedited and formatted. The final version may differ from this version.

2-fold) in $E_2$17G hepatic exposure occurred when $CL_{int,bile}$ was inhibited by 90% because basolateral efflux compensated for impaired biliary excretion. Likewise, $E_2$17G hepatic exposure increased no more than 2.2-fold when $CL_{int,BL}$ was inhibited by 90% due to compensation by biliary excretion. However, up to a 10-fold increase in $E_2$17G hepatic exposure was observed when both $CL_{int,BL}$ and $CL_{int,bile}$ were inhibited simultaneously up to 90% of control values .

9. Discussion

Understanding hepatic $E_2$17G disposition is important because $E_2$17G plays a role in ICP and susceptibility could change if transporter expression is altered by disease or drug interactions. Therefore, this study characterized $E_2$17G disposition in SCHH using the uptake and efflux protocol and mechanistic modeling previously established (Pfeifer et al., 2013) to estimate basolateral uptake and efflux clearance values and biliary excretion clearance. These values were used to study the relative contribution of the different pathways and simulate effects of cholestasis-mediated transporter alterations or drug-drug interactions on hepatic $E_2$17G disposition.

The biliary excretion of $E_2$17G by MRP2 is well documented (Huang et al., 2000; Morikawa et al., 2000). The influence of biliary excretion on $E_2$17G disposition in SCHH is indicated by the BEI, which ranged from 40 - 52% in the three hepatocyte lots. This BEI range for $E_2$17G is in agreement with previously published values of 32 - 43% (Bi et al., 2006; Lee et al., 2010). The mean $E_2$17G $CL_{int,bile}$ estimate determined here (0.11 ml/min/g liver) was similar to TCA $CL_{int,bile}$ (0.14 ml/min/g liver) determined previously (Yang et al., 2015). Whereas TCA is predominantly excreted into bile in SCHH (Yang et al., 2015), this is not the case for $E_2$17G. The $CL_{int,BL}$ of TCA is 3.3-fold lower than $CL_{int,bile}$ (Yang et al., 2015). In contrast, based on our results, the $CL_{int,BL}$ of $E_2$17G is 1.6-fold higher than $CL_{int,bile}$ (Table 2). Thus, basolateral efflux is an important route of $E_2$17G elimination in SCHH. It should be noted that there is inter-donor variability in the ratio of $CL_{int,BL}$ to $CL_{int,bile}$; the ratio is 0.9, 2.0, and 2.8 in hepatocyte Lots 1, 2 and 3, respectively (Table 2). This variability is expected based on large individual differences in protein levels of hepatic efflux transporters. For example, MRP2 and MRP3 protein expression showed 4-fold individual differences in human liver tissue from more than 50 donors (Wang et al., 2015).

At the basolateral membranes of hepatocytes, MRP3 and MRP4 transport substrates from the cells to the sinusoidal blood (Chandra and Brouwer, 2004). Although our data cannot identify the

transporters responsible for the basolateral efflux of $E_2$17G, it is likely to be mediated by MRP3 and/or MRP4, because $E_2$17G is a well-established substrate for these efflux transporters (Zeng et al., 2000; Chen et al., 2001). MRP3 and MRP4 have comparable K_m values for $E_2$17G (Zeng et al., 2000; Chen et al., 2001; Zamek-Gliszczynski et al., 2006). However, in human liver tissue, the absolute protein level of MRP3 is at least 40-fold higher than MRP4 (Vildhede et al., 2015). Thus, MRP3 is assumed to be the primary transporter mediating the hepatic basolateral efflux of $E_2$17G in healthy subjects. It should be noted that $E_2$17G is not a substrate of OSTα/β, which also is expressed on the basolateral membranes of hepatocytes (Malinen et al., 2018).

The contribution of basolateral efflux to $E_2$17G elimination from hepatocytes could be amplified in situations where basolateral efflux transporter levels are increased. Basolateral transporters can be induced in several liver diseases, including cholestasis (Thakkar et al., 2017). For example, MRP3 protein levels increased 4.6-fold in patients with obstructive cholestasis caused by gall stones (Chai et al., 2012), and increased 2.1- to 2.6-fold in patients with stage III/IV primary biliary cirrhosis (Zollner et al., 2003). A similar increase compared to control subjects was reported for MRP4 in obstructive cholestasis (3.1-fold) and primary biliary cirrhosis (3.2 – 3.5-fold) (Zollner et al., 2007; Chai et al., 2011). MRP3 and MRP4 protein levels also are increased in nonalcoholic steatohepatitis (Hardwick et al. 2011). In addition, Mrp3 is upregulated in Mrp2-deficient TR^- rats and in patients with Dubin-Johnson syndrome (Konig et al., 1999; Johnson et al., 2006). In contrast, MRP2 levels do not appear to be changed in cholestasis, but some studies point to a mislocalization of MRP2 in cholestatic disease (Zollner et al., 2001; Kojima et al., 2003; Zollner et al., 2003; Chai et al., 2012).

A sensitivity analysis was performed to evaluate the effects of changes in efflux protein levels on hepatic $E_2$17G disposition. The analysis revealed that hepatic $E_2$17G was sensitive to $CL_{int,BL}$; a 4-fold increase in $CL_{int,BL}$ decreased hepatic $E_2$17G by 64% (Fig. 4A). Biliary $E_2$17G also was examined because $E_2$17G in bile may play a role in the development of cholestasis through trans-

DMD Fast Forward. Published on November 19, 2019 as DOI: 10.1124/dmd.119.088898
This article has not been copyedited and formatted. The final version may differ from this version.

inhibition of BSEP (Stieger et al., 2000). Biliary $E_2$17G was influenced by both basolateral and biliary transporters (Fig. 4B). Sensitivity analysis of $CL_{int,bile}$ revealed that a decrease in $CL_{int,bile}$ (e.g., MRP2 downregulation) effectively decreased the amount of $E_2$17G in bile (Fig. 4B). However, the effects on $E_2$17G accumulation in hepatocytes were smaller (Fig. 4A). Importantly, decreased $CL_{int,bile}$ caused only a minimal increase in cellular $E_2$17G amounts when $CL_{int,BL}$ was induced 4-fold (Fig. 4A). These results suggest that induction of basolateral efflux transporters (e.g., MRP3 and MRP4) in cholestasis could lower the amount of $E_2$17G in hepatocytes, even when biliary clearance is impaired, and may help relieve cholestasis. Pregnant women with defects in these compensatory mechanisms could be predisposed to developing ICP.

The inhibition of MRP3 and MRP4 is a risk factor for drug-induced cholestasis (Morgan et al., 2013; Kock et al., 2014; Chan and Benet, 2018). In addition, MRP2 inhibition alongside possible mislocalization in cholestasis can disturb hepatocellular homeostasis of MRP2 substrates. As expected, our simulations revealed that inhibition of either $CL_{int,BL}$ alone (i.e., MRP3 and MRP4 transport), or inhibition of $CL_{int,bile}$ alone (i.e., MRP2 transport), has a minimal effect on hepatic $E_2$17G exposure (Fig. 5). This is consistent with the concept of fractional excretion (Zamek-Gliszczynski et al., 2009). Based on the calculated clearance estimates in SCHH, 61% of $E_2$17G is excreted via the basolateral pathway. Therefore, even a complete knockout of this predominant excretion pathway would only increase $E_2$17G in hepatocytes by a maximum of 2.6-fold, assuming that no changes in the compensatory biliary pathway occurred. However, simulations indicated that hepatic $E_2$17G was markedly increased with simultaneous inhibition of both pathways (Fig. 5). The simultaneous inhibition of several MRP transporters is a likely event due to overlap in the inhibitor specificity of MRPs (Morgan et al., 2013), and this may predispose patients to $E_2$17G-mediated cholestasis. For example, medications that have been associated with drug-induced liver injury and cholestasis (e.g., repaglinide, cyclosporine A, everolimus) exhibit overlapping inhibition of MRP2, MRP3, and MRP4 (Morgan et al., 2013).

The hepatic clearance estimates of $E_2$17G were determined assuming linear processes. No saturation of these pathways is expected with the 0.3 µM $E_2$17G dose used in this study. The apparent K_m for the uptake clearance of $E_2$17G in plated human hepatocytes is reported to be 7.7 µM (Liao et al., 2018) and the K_m values of $E_2$17G for MRP3 and MRP4 are in the range of 20 – 40 µM determined in vesicle studies (Zeng et al., 2000; Chen et al., 2001; Zamek-Gliszczynski et al., 2006). $E_2$17G shows co-operative binding and sigmoidal kinetics of MRP2-mediated transport in membrane vesicles with K_m/$K_{0.5}$ values of > 100 µM (Heredi-Szabo et al., 2009). The highest hepatocellular concentrations of $E_2$17G reached in this study were < 1.5 µM. Therefore, we believe that the assumption of linearity is reasonable. Another simplification of the model was that passive permeability was not modeled as a separate parameter. However, passive permeability has been shown previously to play a minor role in $E_2$17G uptake in hepatocytes, with active processes contributing to 89.3 ± 8.1% of total uptake (Liao et al., 2018). The biliary excretion of $E_2$17G was decreased by more than 75% in the presence of the MRP2 inhibitor sulindac or its metabolite (Lee et al., 2010), suggesting that passive permeability is also minor in $E_2$17G efflux from hepatocytes.

SCHH continue to be a standard method for assessing hepatic disposition *in vitro*, particularly regarding transporter-mediated efflux (Brouwer et al., 2013). As bile networks re-form over days in culture, the levels of efflux transporters increase and exhibit appropriate functionality (Swift et al., 2010). An important consideration with this study is that levels of individual transporters in SCHH may differ from those in liver tissue, which could limit the ability to accurately translate data from *in vitro* to *in vivo*. Recently, the absolute protein abundance of MRP2 and MRP3, the primary transporters involved in hepatic $E_2$17G efflux, was reported to be ≈ 4-fold higher, on average, in SCHH than in liver tissue from corresponding donors (Kumar et al., 2019). However, the ratio of absolute levels of MRP2 to MRP3 was similar in SCHH and liver tissue (Kumar et al. 2019). Although protein abundance was not determined in the current study, the available literature

suggests that the relative contribution of the efflux pathways of interest are similar in SCHH and in liver tissue.

In summary, this study revealed that basolateral efflux in addition to biliary excretion is a significant route of $E_2$17G elimination in SCHH. The importance of this elimination pathway is further emphasized when basolateral efflux transporter levels (e.g., MRP3 and MRP4) are increased, which may occur in conditions such as cholestasis. The simulations presented here highlight how hepatocytes can effectively cope with increased $E_2$17G through the regulation of both basolateral and biliary transporters.

10. Acknowledgements

The authors gratefully acknowledge Certara for providing Phoenix® software to the UNC Eshelman School of Pharmacy, Division of Pharmacotherapy and Experimental Therapeutics, as part of the Pharsight Academic Center of Excellence Program.

11. Authorship Contributions

Participated in research design: Ito, Brouwer.

Conducted experiments: Ito, Sjöstedt.

Performed data analysis: Ito, Sjöstedt, Brouwer.

Wrote or contributed to the writing of the manuscript: Sjöstedt, Ito, Brouwer.

References

Bi YA, Kazolias D, and Duignan DB (2006) Use of cryopreserved human hepatocytes in sandwich culture to measure hepatobiliary transport. *Drug Metab Dispos* **34:**1658-1665.

Boyer JL, Trauner M, Mennone A, Soroka CJ, Cai SY, Moustafa T, Zollner G, Lee JY, and Ballatori N (2006) Upregulation of a basolateral FXR-dependent bile acid efflux transporter OSTalpha-OSTbeta in cholestasis in humans and rodents. *Am J Physiol Gastrointest Liver Physiol* **290:**G1124-1130.

Brouwer KLR, Keppler D, Hoffmaster KA, Bow DA, Cheng Y, Lai Y, Palm JE, Stieger B, Evers R, and International Transporter C (2013) In vitro methods to support transporter evaluation in drug discovery and development. *Clin Pharmacol Ther* **94:**95-112.

Chai J, He Y, Cai SY, Jiang Z, Wang H, Li Q, Chen L, Peng Z, He X, Wu X, Xiao T, Wang R, Boyer JL, and Chen W (2012) Elevated hepatic multidrug resistance-associated protein 3/ATP-binding cassette subfamily C 3 expression in human obstructive cholestasis is mediated through tumor necrosis factor alpha and c-Jun NH2-terminal kinase/stress-activated protein kinase-signaling pathway. *Hepatology* **55:**1485-1494.

Chai J, Luo D, Wu X, Wang H, He Y, Li Q, Zhang Y, Chen L, Peng ZH, Xiao T, Wang R, and Chen W (2011) Changes of organic anion transporter MRP4 and related nuclear receptors in human obstructive cholestasis. *J Gastrointest Surg* **15:**996-1004.

Chan R and Benet LZ (2018) Measures of BSEP Inhibition In Vitro Are Not Useful Predictors of DILI. *Toxicol Sci* **162:**499-508.

Chandra P and Brouwer KLR (2004) The complexities of hepatic drug transport: current knowledge and emerging concepts. *Pharm Res* **21:**719-735.

Chen ZS, Lee K, and Kruh GD (2001) Transport of cyclic nucleotides and estradiol 17-beta-D-glucuronide by multidrug resistance protein 4. Resistance to 6-mercaptopurine and 6-thioguanine. *J Biol Chem* **276:**33747-33754.

Elferink RO and Groen AK (2002) Genetic defects in hepatobiliary transport. *Biochim Biophys Acta* **1586:**129-145.

Geenes V and Williamson C (2009) Intrahepatic cholestasis of pregnancy. *World J Gastroenterol* **15:**2049-2066.

Hardwick RN, Fisher CD, Canet MJ, Scheffer GL, Cherrington NJ (2011) Variations in ATP-binding cassette transporter regulation during the progression of human nonalcoholic fatty liver disease. *Drug Metab Dispos* **39**: 2395-2402.

Heredi-Szabo K, Glavinas H, Kis E, Mehn D, Bathori G, Veres Z, Kobori L, von Richter O, Jemnitz K, and Krajcsi P (2009) Multidrug resistance protein 2-mediated estradiol-17beta-D-glucuronide transport potentiation: in vitro-in vivo correlation and species specificity. *Drug Metab Dispos* **37:**794-801.

Huang L, Smit JW, Meijer DK, and Vore M (2000) Mrp2 is essential for estradiol-17beta(beta-D-glucuronide)-induced cholestasis in rats. *Hepatology* **32:**66-72.

Johnson BM, Zhang P, Schuetz JD, and Brouwer KLR (2006) Characterization of transport protein expression in multidrug resistance-associated protein (Mrp) 2-deficient rats. *Drug Metab Dispos* **34:**556-562.

Karlgren M, Vildhede A, Norinder U, Wisniewski JR, Kimoto E, Lai Y, Haglund U, and Artursson P (2012) Classification of inhibitors of hepatic organic anion transporting polypeptides (OATPs): influence of protein expression on drug-drug interactions. *J Med Chem* **55:**4740-4763.

Köck K, Ferslew BC, Netterberg I, Yang K, Urban TJ, Swaan PW, Stewart PW, and Brouwer KLR (2014) Risk factors for development of cholestatic drug-induced liver injury: inhibition of hepatic basolateral bile acid transporters multidrug resistance-associated proteins 3 and 4. *Drug Metab Dispos* **42:**665-674.

Kojima H, Nies AT, Konig J, Hagmann W, Spring H, Uemura M, Fukui H, and Keppler D (2003) Changes in the expression and localization of hepatocellular transporters and radixin in primary biliary cirrhosis. *J Hepatol* **39:**693-702.

Konig J, Rost D, Cui Y, and Keppler D (1999) Characterization of the human multidrug resistance protein isoform MRP3 localized to the basolateral hepatocyte membrane. *Hepatology* **29:**1156-1163.

Kumar V, Salphati L, Hop C, Xiao G, Lai Y, Mathias A, Chu X, Humphreys WG, Liao M, Heyward S, and Unadkat JD (2019) A Comparison of Total and Plasma Membrane Abundance of Transporters in Suspended, Plated, Sandwich-Cultured Human Hepatocytes Versus Human Liver Tissue Using Quantitative Targeted Proteomics and Cell Surface Biotinylation. *Drug Metab Dispos* **47:**350-357.

Lee JK, Paine MF, and Brouwer KLR (2010) Sulindac and its metabolites inhibit multiple transport proteins in rat and human hepatocytes. *J Pharmacol Exp Ther* **334:**410-418.

Liao M, Zhu Q, Zhu A, Gemski C, Ma B, Guan E, Li AP, Xiao G, and Xia CQ (2018) Comparison of uptake transporter functions in hepatocytes in different species to determine the optimal model for evaluating drug transporter activities in humans. *Xenobiotica***:**1-11.

Liu X, LeCluyse EL, Brouwer KR, Lightfoot RM, Lee JI, and Brouwer KLR (1999) Use of Ca^{2+} modulation to evaluate biliary excretion in sandwich-cultured rat hepatocytes. *J Pharmacol Exp Ther* **289:**1592-1599.

Malinen MM, Ali I, Bezencon J, Beaudoin JJ, and Brouwer KLR (2018) Organic solute transporter OSTalpha/beta is overexpressed in nonalcoholic steatohepatitis and modulated by drugs associated with liver injury. *Am J Physiol Gastrointest Liver Physiol* **314:**G597-G609.

Miszczuk GS, Barosso IR, Larocca MC, Marrone J, Marinelli RA, Boaglio AC, Sanchez Pozzi EJ, Roma MG, and Crocenzi FA (2018) Mechanisms of canalicular transporter endocytosis in the cholestatic rat liver. *Biochim Biophys Acta Mol Basis Dis* **1864:**1072-1085.

Morgan RE, van Staden CJ, Chen Y, Kalyanaraman N, Kalanzi J, Dunn RT, 2nd, Afshari CA, and Hamadeh HK (2013) A multifactorial approach to hepatobiliary transporter assessment enables improved therapeutic compound development. *Toxicol Sci* **136:**216-241.

Morikawa A, Goto Y, Suzuki H, Hirohashi T, and Sugiyama Y (2000) Biliary excretion of 17beta-estradiol 17beta-D-glucuronide is predominantly mediated by cMOAT/MRP2. *Pharm Res* **17:**546-552.

Mottino AD, Cao J, Veggi LM, Crocenzi F, Roma MG, and Vore M (2002) Altered localization and activity of canalicular Mrp2 in estradiol-17beta-D-glucuronide-induced cholestasis. *Hepatology* **35:**1409-1419.

Musey PI, Wright K, Preedy JRK, and Collins DC (1997) Formation and metabolism of steroid conjugates: effect of conjugation on excretion and tissue distribution, in: *Steroid Biochemistry* (Hobkirk R ed), CRC Press.

Pedersen JM, Matsson P, Bergstrom CA, Norinder U, Hoogstraate J, and Artursson P (2008) Prediction and identification of drug interactions with the human ATP-binding cassette transporter multidrug-resistance associated protein 2 (MRP2; ABCC2). *J Med Chem* **51:**3275-3287.

Pfeifer ND, Yang K, and Brouwer KLR (2013) Hepatic basolateral efflux contributes significantly to rosuvastatin disposition I: characterization of basolateral versus biliary clearance using a novel protocol in sandwich-cultured hepatocytes. *J Pharmacol Exp Ther* **347:**727-736.

Slikker W, Jr., Vore M, Bailey JR, Meyers M, and Montgomery C (1983) Hepatotoxic effects of estradiol-17 beta-D-glucuronide in the rat and monkey. *J Pharmacol Exp Ther* **225:**138-143.

Sohlenius-Sternbeck AK (2006) Determination of the hepatocellularity number for human, dog, rabbit, rat and mouse livers from protein concentration measurements. *Toxicol In Vitro* **20:**1582-1586.

Stieger B, Fattinger K, Madon J, Kullak-Ublick GA, and Meier PJ (2000) Drug- and estrogen-induced cholestasis through inhibition of the hepatocellular bile salt export pump (Bsep) of rat liver. *Gastroenterology* **118:**422-430.

Swift B, Pfeifer ND, and Brouwer KLR (2010) Sandwich-cultured hepatocytes: an in vitro model to evaluate hepatobiliary transporter-based drug interactions and hepatotoxicity. *Drug Metab Rev* **42:**446-471.

Takikawa H, Sano N, Narita T, Uchida Y, Yamanaka M, Horie T, Mikami T, and Tagaya O (1991) Biliary excretion of bile acid conjugates in a hyperbilirubinemic mutant Sprague-Dawley rat. *Hepatology* **14:**352-360.

Thakkar N, Slizgi JR, and Brouwer KLR (2017) Effect of Liver Disease on Hepatic Transporter Expression and Function. *J Pharm Sci* **106:**2282-2294.

Vallejo M, Briz O, Serrano MA, Monte MJ, and Marin JJ (2006) Potential role of trans-inhibition of the bile salt export pump by progesterone metabolites in the etiopathogenesis of intrahepatic cholestasis of pregnancy. *J Hepatol* **44:**1150-1157.

Vildhede A, Wisniewski JR, Noren A, Karlgren M, and Artursson P (2015) Comparative Proteomic Analysis of Human Liver Tissue and Isolated Hepatocytes with a Focus on Proteins Determining Drug Exposure. *J Proteome Res* **14:**3305-3314.

Walker IA, Nelson-Piercy C, and Williamson C (2002) Role of bile acid measurement in pregnancy. *Ann Clin Biochem* **39:**105-113.

Wang L, Prasad B, Salphati L, Chu X, Gupta A, Hop CE, Evers R, and Unadkat JD (2015) Interspecies variability in expression of hepatobiliary transporters across human, dog, monkey, and rat as determined by quantitative proteomics. *Drug Metab Dispos* **43:**367-374.

Yang K, Pfeifer ND, Kock K, and Brouwer KLR (2015) Species differences in hepatobiliary disposition of taurocholic acid in human and rat sandwich-cultured hepatocytes: implications for drug-induced liver injury. *J Pharmacol Exp Ther* **353:**415-423.

Zamek-Gliszczynski MJ, Kalvass JC, Pollack GM, and Brouwer KLR (2009) Relationship between drug/metabolite exposure and impairment of excretory transport function. *Drug Metab Dispos* **37:**386-390.

Zamek-Gliszczynski MJ, Hoffmaster KA, Nezasa K, Tallman MN, Brouwer KLR (2006) Integration of hepatic drug transporters and phase II metabolizing enzymes: Mechanisms of hepatic excretion of sulfate, glucuronide, and glutathione metabolites. *Eur J Pharm Sci* **27:**447-486.

Zeng H, Liu G, Rea PA, and Kruh GD (2000) Transport of amphipathic anions by human multidrug resistance protein 3. *Cancer Res* **60:**4779-4784.

Zollner G, Fickert P, Silbert D, Fuchsbichler A, Marschall HU, Zatloukal K, Denk H, and Trauner M (2003) Adaptive changes in hepatobiliary transporter expression in primary biliary cirrhosis. *J Hepatol* **38:**717-727.

Zollner G, Fickert P, Zenz R, Fuchsbichler A, Stumptner C, Kenner L, Ferenci P, Stauber RE, Krejs GJ, Denk H, Zatloukal K, and Trauner M (2001) Hepatobiliary transporter expression in percutaneous liver biopsies of patients with cholestatic liver diseases. *Hepatology* **33:**633-646.

Zollner G, Wagner M, Fickert P, Silbert D, Gumhold J, Zatloukal K, Denk H, and Trauner M (2007) Expression of bile acid synthesis and detoxification enzymes and the alternative bile acid efflux pump MRP4 in patients with primary biliary cirrhosis. *Liver Int* **27:**920-929.

13. Footnotes

This work was supported by the National Institute of General Medical Sciences of the National Institutes of Health (NIH) [Award Number R35 GM122576] (K.L.R.B.) and by Teijin Pharma Limited. Dr. Sjöstedt was supported by the Sigrid Jusélius Foundation.

Dr. Kim Brouwer is a co-inventor of the sandwich-cultured hepatocyte technology for quantification of biliary excretion (B-CLEAR®) and related technologies, which have been licensed exclusively to Qualyst Transporter Solutions, recently acquired by BioIVT. B-CLEAR® is covered by U.S. patent 6,780,580 and other U.S. and international patents both issued and pending.

This work was presented, in part, at the AAPS 2018 PharmSci 360.

14. Figure Legends

Figure 1. Scheme depicting the uptake and efflux studies performed in sandwich-cultured human hepatocytes (SCHH) with $E_2$17G. A) Test compound ($E_2$17G) is taken up into the cells via uptake transporters (CL_{uptake}) and excreted from the cell to the medium by transporters on the basolateral membrane ($CL_{int,BL}$) or into the bile by canalicular transporters ($CL_{int,bile}$). In the presence of Ca^{2+}, $E_2$17G accumulates in the bile canaliculi, but can flux into the medium (K_{flux}) with contractions of the canaliculi. When incubated in Ca^{2+}-free buffer, the tight junctions of the bile canaliculi are disrupted and all excreted compound returns to the buffer. B) Summary of the SCHH uptake and efflux study protocol performed in the presence and absence of Ca^{2+} to determine biliary excretion.

Figure 2. Estradiol-17β-glucuronide ($E_2$17G) mass (pmol/mg protein) versus time data in sandwich-cultured human hepatocytes (SCHH) during the uptake and efflux phase. SCHH were incubated with [^{3}H] 0.3 µM $E_2$17G (2 µCi/ml) according to the scheme presented in Fig 1B. The simulated mass-time profiles were generated using the relevant equations based on the model scheme depicted in Figure 1A; the final parameter estimates are reported in Table 2. Data are presented as the mean ± SD (n= 3 wells, except n=2 for cell lysate sample in Lot 1 at 0.5 min with Ca^{2+}-free HBSS).

Figure 3. Biliary excretion of estradiol-17β-glucuronide ($E_2$17G) and taurocholate (TCA) in sandwich-cultured human hepatocytes (SCHH). Accumulation (mean ± SD; n = 3) of substrate in SCHH after incubation with 0.3 µM [^{3}H]-$E_2$17G (0.7 µCi/ml) or 1 µM [^{3}H]-TCA (0.8 µCi/ml) for 10 min in standard HBSS after a 10 min preincubation in standard HBSS (black bars; cells+bile) or Ca^{2+}-free HBSS (white bars; cells). The biliary excretion index (BEI, %) was calculated according to Equation 1.

Figure 4. Effects of alterations in intrinsic basolateral efflux clearance ($CL_{int,BL}$) and intrinsic biliary excretion clearance ($CL_{int,bile}$) on estradiol-17β-glucuronide ($E_2$17G) disposition in sandwich-cultured human hepatocytes (SCHH). The impact of designated fold changes in clearance estimates on mean steady-state levels of $E_2$17G in (A) cells and (B) bile, and on (C) the biliary excretion index (BEI) at 10 min are plotted. All values were normalized to control simulations run using the average clearance estimates of $E_2$17G from the mechanistic modeling.

Figure 5. Effects of 0 to 90% efflux inhibition on hepatic $E_2$17G exposure. The hepatocyte to buffer concentration ratio (K_p, Equation 7) was calculated using average clearance values (control) and decreasing either the intrinsic basolateral efflux clearance ($CL_{int,BL}$) and/or biliary excretion clearance ($CL_{int,bile}$). Exposure is shown as fold change from control (no inhibition). When $CL_{int,bile}$ is inhibited by 90%, hepatic $E_2$17G exposure is 1.5-fold (point A). When $CL_{int,BL}$ is inhibited by 90%, hepatic $E_2$17G exposure is 2.2-fold (point B). However, when both $CL_{int,bile}$ and $CL_{int,BL}$ are inhibited by 90%, the hepatic $E_2$17G exposure increases 10-fold (point C).

15. Tables

Table 1. Donor information for the three hepatocyte lots used in the studies. All donors were female.

	Lot 1	**Lot 2**	**Lot 3**
Race	Caucasian	Caucasian	Caucasian/Hispanic
Age (years)	37	55	44
BMI (kg/m^2)	22	24	29
Cause of death	Head trauma	Stroke	Anoxia, cerebrovascular accident

DMD Fast Forward. Published on November 19, 2019 as DOI: 10.1124/dmd.119.088898
This article has not been copyedited and formatted. The final version may differ from this version.

Table 2. Final parameter estimates from the model fitting.

Hepatocyte lot	CL_{uptake}	$CL_{int,BL}$	$CL_{int,bile}$	K_{flux}
	ml/min/g liver (CV%)			min^{-1} (CV%)
Lot 1	0.69 (15%)	0.16 (68%)	0.18 (47%)	0.31 (41%)
Lot 2	1.2 (9%)	0.17 (19%)	0.083 (35%)	0.21 (22%)
Lot 3	0.98 (9%)	0.21 (14%)	0.073 (28%)	0.17 (22%)
Mean ± SD	0.96 ± 0.26	0.18 ± 0.03	0.11 ± 0.06	0.23 ± 0.07

DMD Fast Forward. Published on November 19, 2019 as DOI: 10.1124/dmd.119.088898
This article has not been copyedited and formatted. The final version may differ from this version.

Figure 1:

A.

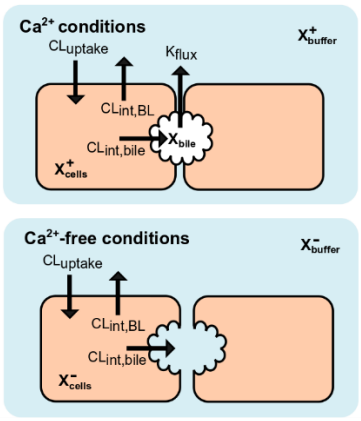

B.

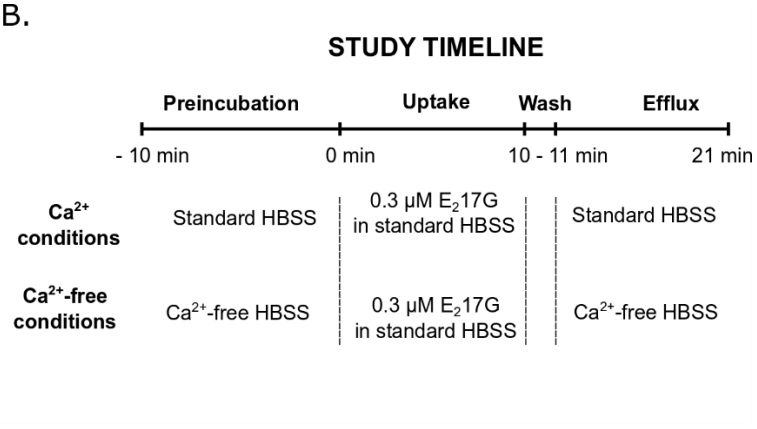

DMD Fast Forward. Published on November 19, 2019 as DOI: 10.1124/dmd.119.088898
This article has not been copyedited and formatted. The final version may differ from this version.

Figure 2:

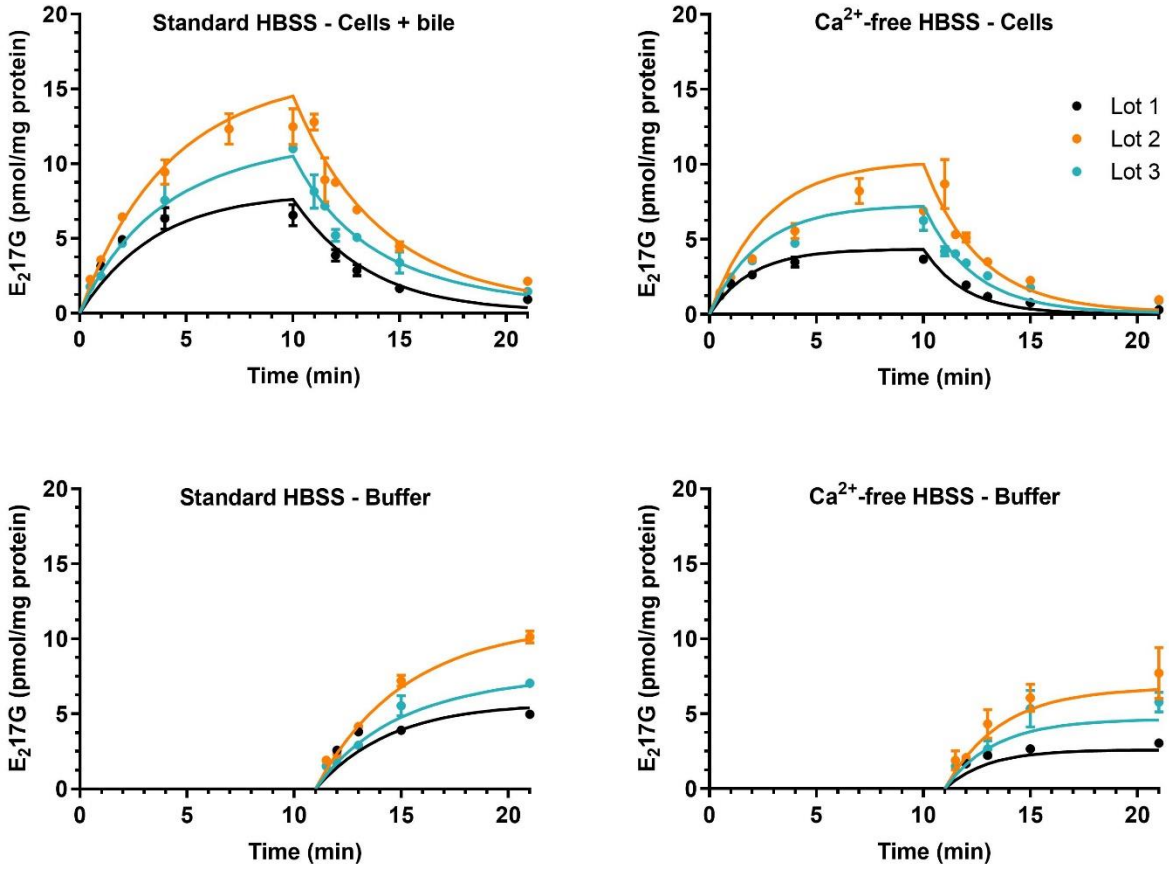

DMD Fast Forward. Published on November 19, 2019 as DOI: 10.1124/dmd.119.088898
This article has not been copyedited and formatted. The final version may differ from this version.

Figure 3:

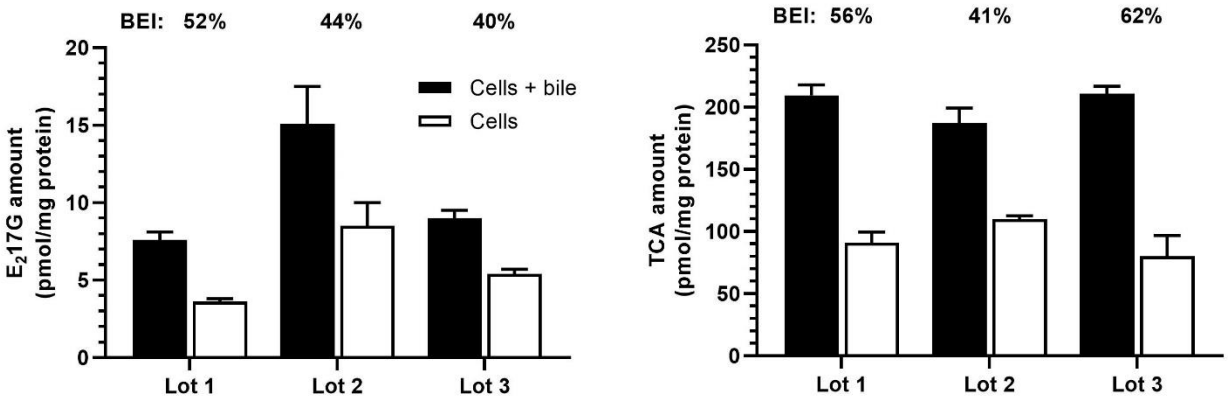

DMD Fast Forward. Published on November 19, 2019 as DOI: 10.1124/dmd.119.088898
This article has not been copyedited and formatted. The final version may differ from this version.

Figure 4:

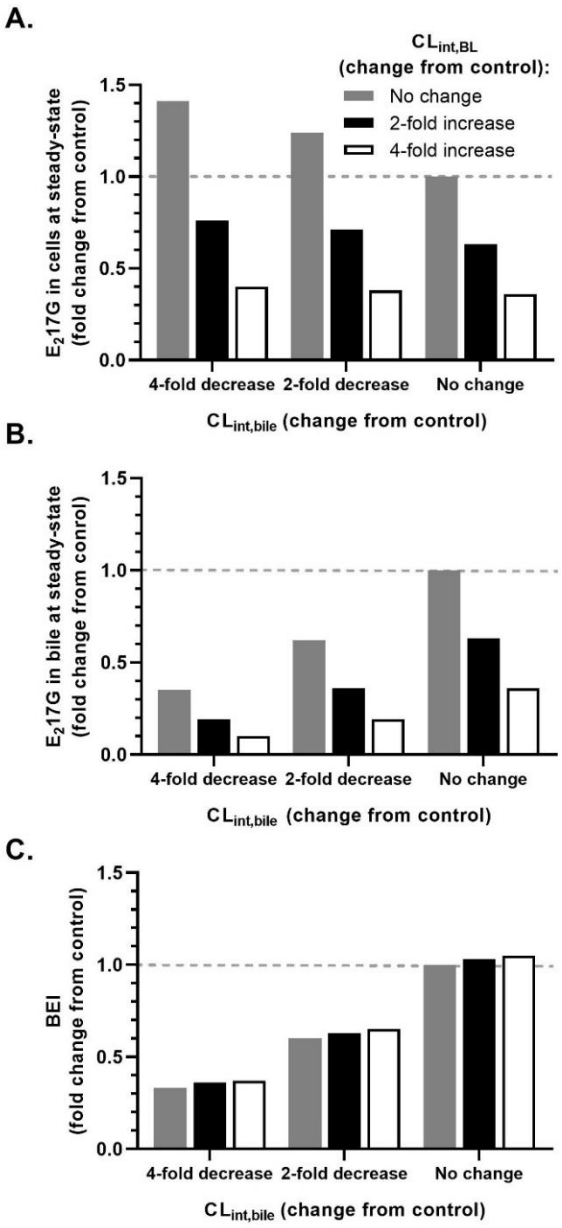

DMD Fast Forward. Published on November 19, 2019 as DOI: 10.1124/dmd.119.088898
This article has not been copyedited and formatted. The final version may differ from this version.

Figure 5: